Research & Reviews: Journal of Material Sciences
DOI: 10.4172/2321-6212.1000242

e-ISSN: 2321-6212
p-ISSN: 2347-2278

Ionizing Radiation Effect on the Catalytic Properties of Cerium Oxide Nanoparticles

Mai M El-Masry[1]*, Ahmed MA[2] and Bishay ST[3]

[1]Basic Science Department, Higher Engineering Institute, Thebes Academy, Egypt

[2]Physics Department, Faculty of Science, Materials Science Lab, Cairo University, Egypt

[3]Physics Department, Faculty of Girls for Arts, Science and Education, Ain Shams University, Egypt

Research Article

Received: 23/07/2018
Accepted: 02/06/2019
Published: 02/13/2019

***For Correspondence**

Mai M EL-Masry, Basic science Department, Higher Engineering Institute, Thebes Academy, Egypt

Tel: 20 2 25247984

E-mail: mai.elmasry@thebes.edu.eg

Keywords: Cerium oxide nanoparticles, Ionizing radiation, Catalytic properties, Relative fraction (%) of Ce^{3+}

ABSTRACT

Cerium oxide nanoparticles have unique catalytic properties which make it a promising regenerative and a great free radical scavenger especially in the biomedical applications. Cerium oxide catalytic properties are affected by the relative fraction (%) of Ce^{3+} which in turn depends on the particle size.

In the preset work, the catalytic properties of cerium oxide have been improved by increasing the relative fraction (%) of Ce^{3+}. In order to reach this goal cerium oxide has been prepared in the nano-scale and the effect of treating these prepared nanoparticles by ionizing radiation of each cold plasma and gamma on the relative fraction (%) of Ce^{3+} has been studied.

INTRODUCTION

Cerium (Ce) has electronic configuration $[Xe]4f^26s^2$ and has two common oxidation states Ce^{3+} and Ce^{4+} In cerium dioxide form it adopts cubic fluorite crystal structure and displays a range of interesting physical and chemical properties such as strong UV-absorption [1,2], high optical transparency in the visible region [2], high refractive index, interesting redox properties, high oxygen storage- and releasing capacity [1-4]. This is why it is a highly promising material for a wide range of applications such as electrolytes in solid oxide fuel cells, UV-filter,fuel additives, solar cells and catalytic material [5-9].

In all these applications, the high performance of CeO_2 NPs is attributed to their rich Oxygen vacancies and low redox potential [10,11]. It is well known that O vacancies are formed due to the highly mobile nature of the surface oxygen [12,13]. Two excess electrons, left behind by the formation of O vacancies, are localized on the 4f-state of the nearest Ce ions, leading to a valence change in the Ce ions from Ce^{4+} to Ce^{3+} [14,15].

Many nanoparticles are being studied to test their possible application in biomedical therapy; among these, cerium oxide nanoparticles (CeNPs) are being proven promising for their regenerative, scavenging of reactive oxygen species (ROS) [16-18]. CeNPs' unique antioxidant/catalytic properties stem from, the coexistence of oxidation states 3+ (Ce^{3+}) and 4+ (Ce^{4+}), the reversible switching between these states and the low reduction potential of ~1.52 V [17].

Cerium dioxide as a bulk crystal mainly consists of Ce^{4+}, but reduction in size to nano-dimensions significantly enhances the relative amount of the relative fraction of Ce^{3+} resulting in higher catalytic effects which are comparable to the capabilities of biological antioxidants and highly relevant for biological processes [19,20].

CeNPs capability to switch in anti-/pro-oxidant properties can be utilized for sensitizing cancer cells for radiation therapy while protecting normal cells, neuroprotective, cell longevity-enhancing, and anti-inflammatory properties [21,22].

e-ISSN: 2321-6212
p-ISSN: 2347-2278

In this work we tried to increase the (Ce^{3+}) relative fraction to improve the catalytic performance of cerium oxide by decreasing the particle size of the prepared samples to the nano-scale.

On the other hand, the relative fraction of (Ce^{3+}) of the prepared nanoparticles were investigated when the samples have treated with ionizing radiation of each plasma and gamma radiation.

Among various types of plasmas, cold plasmas do not cause thermal damage to surfaces they may come in contact with [23].

Today, low temperature plasmas encompass several applications in biology and medicine [24-26]. These include: Sterilization, disinfection, and decontamination, plasma-aided wound healing, plasma dentistry, cancer applications or "plasma oncology," plasma pharmacology, plasma treatment of implants for biocompatibility.

Investigators reported that the effects of low temperature plasma on biological cells are mediated by reactive oxygen and nitrogen species (RONS) [27].

Recently the application that receiving much attention is the use of low temperature plasma to destroy cancer cells and tumors in a selective manner [28].

Gamma rays are used for diagnostic purposes in nuclear medicine in imaging techniques. Anna Giovanetti, et al. have been studied the mechanistic analysis of the potential effects of nanoceria against the detrimental effects of ionizing radiation, and they found that nanoceria strongly protects irradiated cells against immediate damage, to an extent similar to the most potent antioxidants tested. Moreover, nanoceria apparently is able to clear the population of cells surviving X-irradiation from mutation, by impeding survival and propagation of the damaged cells [29].

EXPERIMENTAL SECTION

Sample Preparations

Cerium (III) nitrate ($Ce(NO_3)_3{\cdot}6H_2O$) was chosen as the precursor to prepare ceria samples by a co-precipitation method. Some drops of ammonium hydroxide NH_4OH 33% were added to aqueous solution of cerium nitrate until pH 7.4, and a purple color start to appear in the solution turned in few minutes to a yellowish white precipitation. The collected precipitated cerium oxide nanoparticles were washed several times with deionized water, methanol and ethanol. The precipitated particles were separated using a centrifuge (3500 rpm for 45 minutes). A yellowish white powder of cerium oxide was obtained by drying the collected materials at 70°C for 2 h.

Plasma Irradiation Technique

The samples were irradiated using d.c. pseudo plasma system as shown in **Figures 1a and 1b**. The discharge cell is a Pyrex cylinder with a 6 cm inner diameter and 30 cm long. The cathode is a stainless steel placed in a Pyrex sleeve. The anode is a steel mesh with 30 holes per square inch and is placed at the distance of 4 mm from the cathode. The discharge volume was pumped to about 1.3 Pa (10^{-2} Torr). Its pressure, P, was controlled by a needle valve. The discharge was sustained by using a DC power supply of 1 kV, using currents up to 50 mA. The cathode was connected to the negative potential terminal of the power supply, whereas the anode was at the ground potential.

Small amount of the prepared ceria powder was dispersed in distilled water and then deposited on a glass strip until it is get dried then placed in contact of the anode and exposed to the plasma.

The effect of plasma exposure time, the current of the plasma tube and the pressure of the plasma tube on the prepared samples have been investigated, where

1. The samples were exposed to plasma in exposure time of 15 min, 30 min and 1 h at constant pressure (2 torr) and current (30 mA).
2. Each sample was irradiated for 30 min with the same current of 30 mA and different pressure values of (2, 4, 8 and 12 torr).
3. Each sample was irradiated for 30 min with the same pressure of 2 torr and different current values of (15, 30, 40 and 50 mA) **(Figures 1a and 1b)**.

Research & Reviews: Journal of Material Sciences
DOI: 10.4172/2321-6212.1000242
e-ISSN: 2321-6212
p-ISSN: 2347-2278

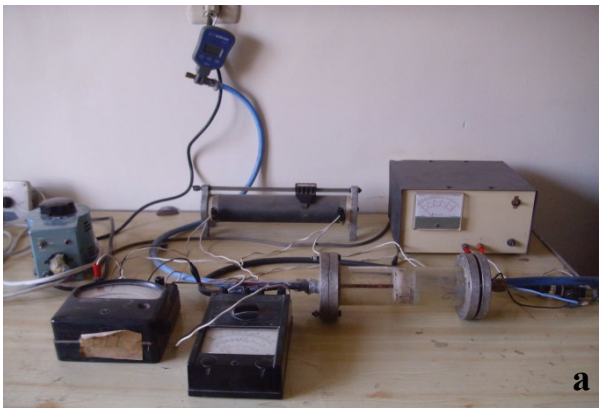

Figure 1a: Set up of plasma pseudo-discharge.

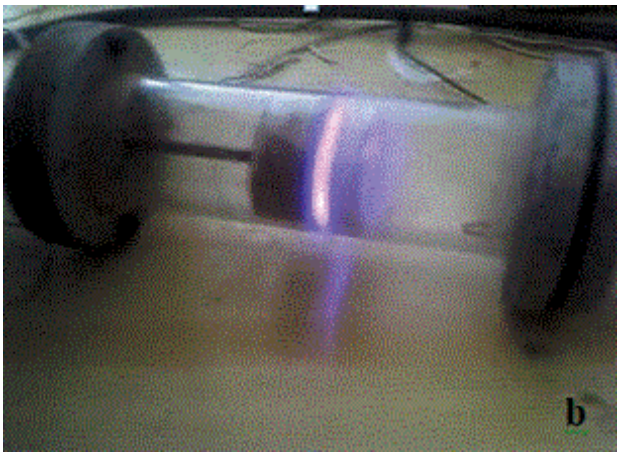

Figure 1b: plasma discharged cell.

Gamma Irradiation Technique

The prepared ceria powder samples were irradiated by γ-rays of 60Co radioactive source at room temperature using irradiation cell (medical sterilizer type CM-20) in the cyclotron facility, Nuclear Research Center, Atomic Energy Authority, Cairo, Egypt. The total exposure dose was (1, 2, 3, 4, 5 Gy) each sample for 10 sec. The irradiated samples were measured using the mentioned device to study the effect of γ-irradiation on the properties of the prepared samples of nano Cerium oxide.

Characterization of the as Prepared and Irradiated Samples

X-ray diffraction (XRD): Proker D_g advance X-ray diffractometer with CuKα radiation (λ=1.5418 Å) has been used to assure the preparation of the cerium oxide in single phase. X-ray diffraction pattern was recorded at room temperature in a wide range of Bragg angles 2θ (20° ≤ 2θ ≤ 80°) with 0.02° step size.

From XRD analysis the crystallite size was calculated according to Scherrer's equation as follows [18,19]:

$$D = \frac{K.\lambda}{\beta.\cos\theta} \quad (1)$$

Where, D is the crystallite size (nm), K is the particle shape factor, taken as 0.94 for cerium oxide [20], λ is the target wavelength (nm), β is the corrected full-width at half maximum, and θ is the position (angle) of the peak at the maximum.

X-ray photoelectron spectroscopy (XPS): XPS spectra were obtained using X-ray photoelectron spectrometer (model Thermo Scientific K-Alpha) with a monochromatic X-ray source of AlKα. The acquisition time is 10 min for all samples, number scans were 20, spot size of 400 μm, lens mode was standard, analyzer mode (CAE: Pass Energy 50.0 eV) with energy step size of 0.100 eV and number of energy steps 601.

RESULTS AND DISCUSSION

Cold Plasma Effect on the Prepared Samples

The prepared sample has been irradiated using pseudo plasma. The effects of the irradiation time and the conditions controlling the plasma beam of each current and pressure on the sample have been investigated.

Research & Reviews: Journal of Material Sciences
DOI: 10.4172/2321-6212.1000242
e-ISSN: 2321-6212
p-ISSN: 2347-2278

Characterization of samples phases: The prepared sample has been irradiated using pseudo plasma for 15 min, 30 min and 60 min at constant pressure of 2 torr and current of 30 mA.

Effect of irradiation time on ceria samples phases - XRD: From XRD analysis the crystallite size was calculated according to Scherrer's equation as follows [30,31]:

$$D = \frac{K.\lambda}{\beta.\cos\theta} \quad (2)$$

Where, D is the crystallite size (nm), K is the particle shape factor, taken as 0.94 for cerium oxide [32], λ is the target wavelength (nm), β is the corrected full-width at half maximum, and θ is the position (angle) of the peak at the maximum.

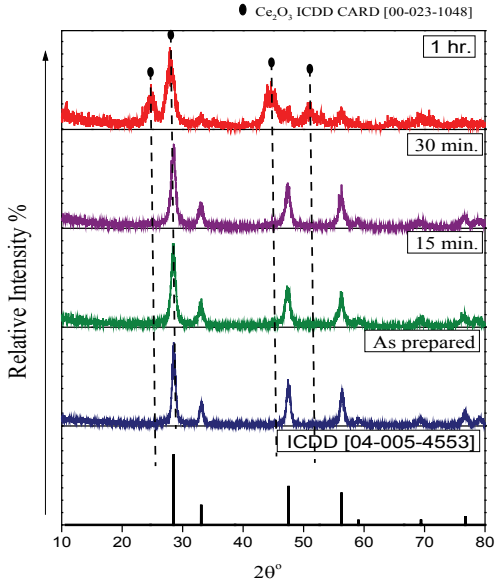

Figure 2: XRD of the cerium oxide exposed to plasma of ionization current 30 (mA) under pressure 2 torr at different time intervals.

Figure 2 shows single phase formation of cerium oxide (CeO_2) nanoparticles of cubic crystal structure when compared to the ICDD card [04-005-4553] for samples exposed to plasma for 15 and 30 min.

The sample irradiated for 60 min showed different XRD pattern with peaks could be compared to the ICDD card [00-023-1048] of the hexagonal cerium oxide (Ce_2O_3). After the irradiation of 60 min higher intensity of electrons reached the sample. These electrons may cause change in the cubic crystal structure. As reported by G. Renu et al. this residual stress shifts nominally reflection from certain planes from the expected 2θ values. In other words for low pressure plasmas, ions are accelerated toward the sample could break the chemical bonds formed between atoms of the material [33]. Therefore, ion bombardment may remove atoms from occupied active sites, create new sites (by creating defects) or even modify structure of the surface.

Effect of the plasma discharge current on the irradiated samples: Figure 3 Clarifies the XRD pattern of the prepared sample exposed to plasma with different cell current at constant pressure (2 torr) and time (30 min). The increase of the plasma cell current increases the electrons flow that hits the sample particles. Gradually the hexagonal cerium oxide (Ce_2O_3) of higher Ce^{3+}% relative fraction discussed in above section start to appear and increases with an increasing the current value.

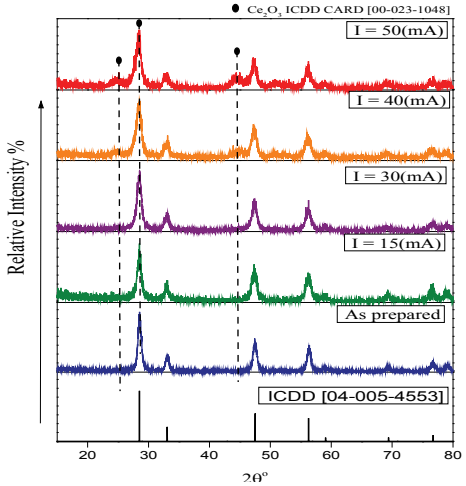

Figure 3: XRD of the cerium oxide exposed to plasma of different ionization current under constant pressure 2 torr at time interval 30 min.

Research & Reviews: Journal of Material Sciences
DOI: 10.4172/2321-6212.1000242
e-ISSN: 2321-6212
p-ISSN: 2347-2278

Effect of the plasma's tube pressure on the irradiated samples: The increase in the cell pressure at constant current value didn't affect the crystallite phase in the range from 2 torr to 12 torr and the sample had the same cubic structure in this pressure range as shown in **Figure 4**. This is could be due to that this range of pressure is not enough to accelerate sufficient density of ions stream which leads to the deformation of the irradiated particles in the investigated samples.

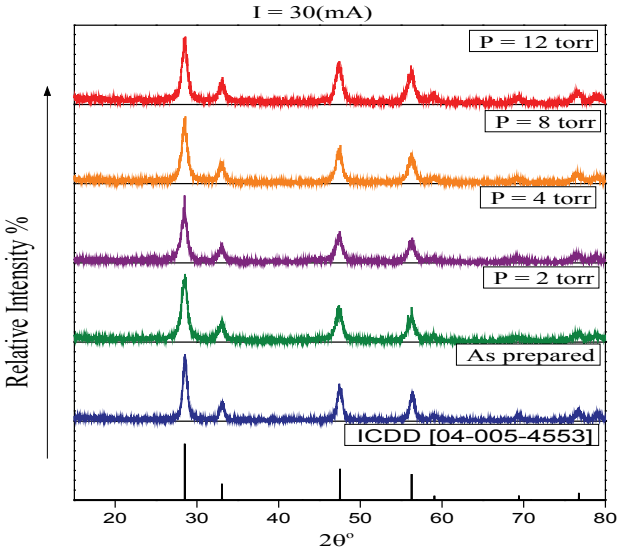

Figure 4: XRD of the cerium oxide exposed to plasma at ionization current 30 (mA) under different pressure values at time interval 30 min.

Oxidation state of samples irradiated by plasma: The XPS pattern in the range of (930-870 ev) of the surface atoms binding energy has been studied to evaluate the percentage of both oxidation states of the investigated samples.

The XPS spectra were deconvoluted as shown in **Figure 5**. The relative fraction (%) of Ce^{3+}were calculated from the integrated areas under the peaks and substituting in the following equation [34].

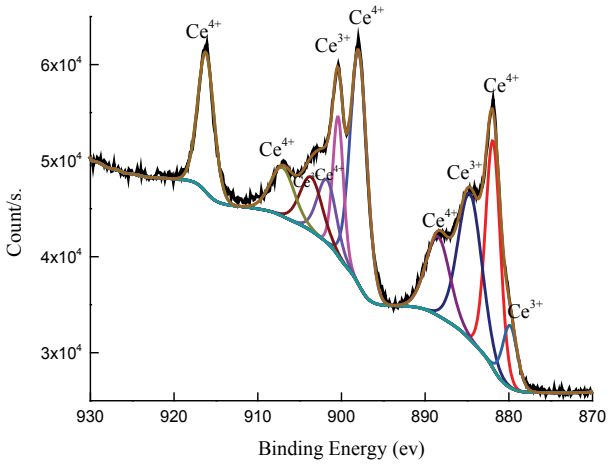

Figure 5: The deconvoluted XPS spectrum of cerium oxide sample.

$$\left[Ce^{3+}\right]\% = \frac{Ce^{3+}}{Ce^{3+} + Ce^{4+}} \quad (3)$$

The relative fraction (%) of Ce^{3+} for the different prepared samples have been examined using the XPS technique in order to obtain the preparation conditions produce the higher relative fraction (%) of Ce^{3+}.

The oxidation state and the relative fraction (%) of Ce^{3+} of the prepared samples exposed to plasma for different time intervals have been estimated.

Research & Reviews: Journal of Material Sciences
DOI: 10.4172/2321-6212.1000242
e-ISSN: 2321-6212
p-ISSN: 2347-2278

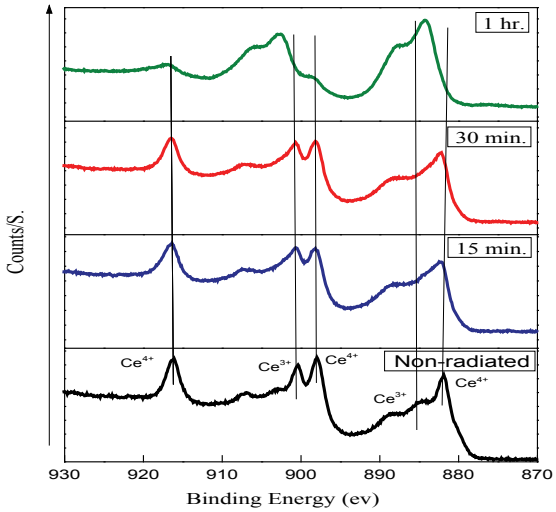

Figure 6a: XPS of cerium oxide Exposed to plasma for different time intervals.

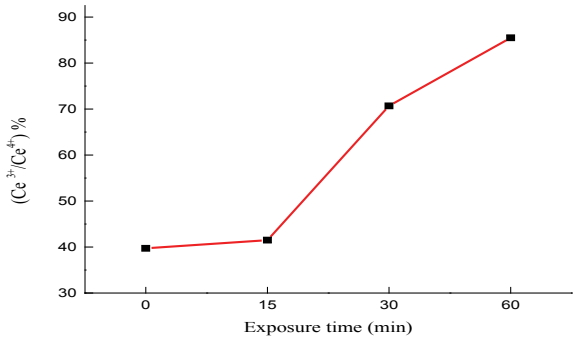

Figure 6b: The change of the calculated relative faction of Ce^{3+}% with time of exposure.

Table 1, Figures 6a and 6b clarified that the increasing of the exposure time of the ceria samples to plasma, increases the relative fraction (%) of Ce^{3+} to about 85%.

This is coincidence with the XRD pattern in **Figure 2** where exposing the sample for time interval of 1 h increases the defects and the oxygen vacancies.

Table 1: Relative fraction (%) of Ce^{3+} for plasma exposed samples for different time intervals.

Exposure time (min)	0	15	30	60
Relative fraction(%) of Ce^{3+}	39.73	41.53	70.73	85.49

Cerium Oxide Samples Irradiated by Gamma Rays with Different Doses

Characterization of samples' phases irradiated by gamma rays with different doses - XRD: In the present work the effect of gamma rays on the physical and structural properties has been studied.

Nao-ceria was exposed to gamma rays of doses in range of (1-5 Gy), the range of the radiotherapy doses.

Research & Reviews: Journal of Material Sciences
DOI: 10.4172/2321-6212.1000242
e-ISSN: 2321-6212
p-ISSN: 2347-2278

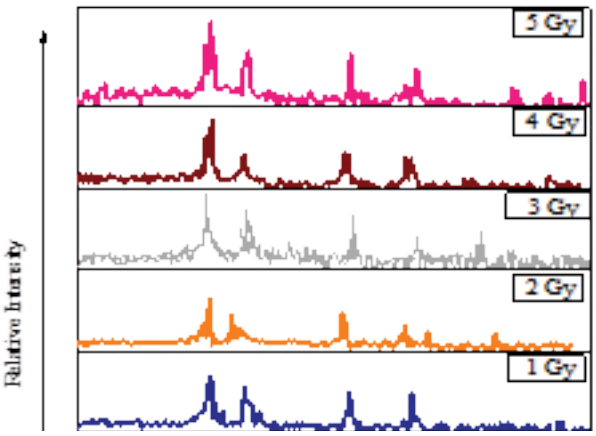

Figure 7: XRD of the cerium oxide irradiated by gamma rays with different doses.

Figure 7 showed the XRD pattern of the prepared sample compared to the same sample irradiated by gamma rays for (16 seconds) of doses (1, 2, 3,4 and 5 Gy). The irradiated samples showed very poor sharp peaks with noise percentage compared to the non-radiated sample. This is could be a result of the effect of high power radiation (gamma) which produced crystal distortion and lower symmetry of the unit cell of the nano-ceria.

Oxidation state of ceria samples irradiated by gamma rays with different doses: From **Table 2, Figures 8a and 8b** it can be seen that gamma rays had increased the relative fraction (%) of Ce^{3+} when exposed to dose of (1 Gy), this percentage didn't affect badly until the sample exposed to the highest dose of (5 Gy). This could be a result of the interaction of the gamma rays with the cerium oxide material.

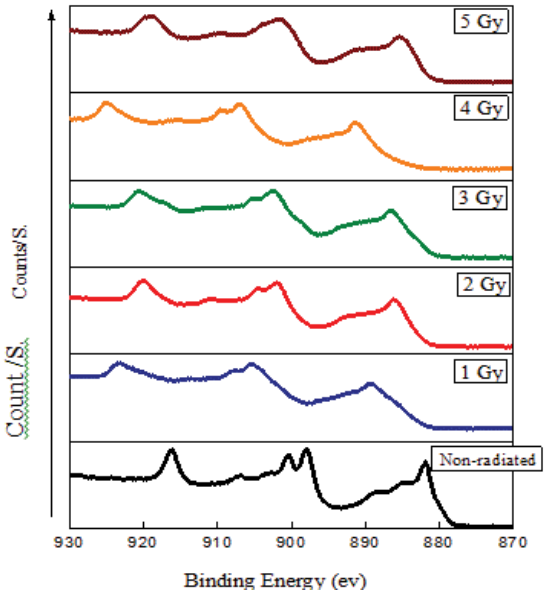

Figure 8a: XPS of cerium oxide Exposed to gamma for different doses.

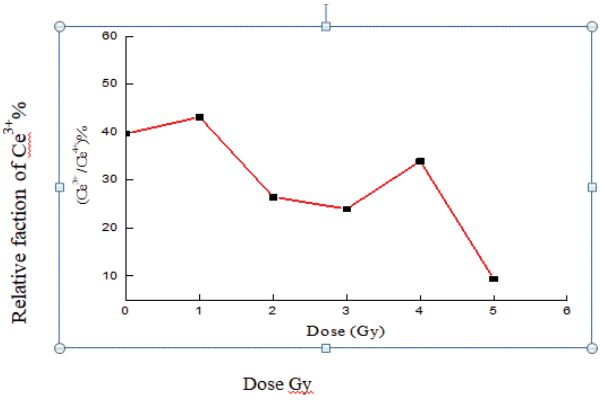

Figure 8b: Relative faction of Ce^{3+}% change with the exposure dose.

e-ISSN: 2321-6212
p-ISSN: 2347-2278

The interaction resulted from either Compton effect or photoelectron effect. Compton effect, where gamma transfer its energy to the electrons which not bound tightly enough to the atom. In the photoelectric effect, some of the gamma ray's energy is used to overcome the electron binding energy and the remainder is transferred to the freed electron as a kinetic energy [23]. Both interactions cause the cerium oxide samples to lose electron. This is led to a decrease in the relative fraction (%) of Ce^{3+}, free radical scavenging ability, and damage the cerium oxide crystal structure **(Table 2)**.

Table 2: Relative fraction (%) of Ce^{3+} for gamma irradiated samples with different doses.

Exposure dose (Gy)	Nonradiated	1	2	3	4	5
Relative fraction (%) of Ce^{3+}	39.73	43.19	26.5	24.02	33.99	9.39

CONCLUSION

Cerium oxide has been prepared in the nano scale and the particle sizes have been examined using (XRD) technique. The prepared nano particles have been exposed to ionizing radiation of each plasma and γ-radiation.

The estimated results showed that,

- The catalytic performance and the relative fraction (%) of Ce^{3+} has been improved when the prepared cerium oxide nano-particles treated with cold plasma for about 60 min.
- Also the relative fraction (%) of Ce^{3+} has been increased as the plasma's tube current was minimum 30 mA.
- Nano-ceria is suitable to use in the Gamma rays applications especially in the radiotherapy as a free radical scavenger where, the relative fraction (%) of Ce^{3+} was not affected badly by the gamma rays except for the largest dose (5 Gy).
- The investigated samples when treated with different doses of gamma radiation, showed very poor crystallinity and a structure deformation because of the gamma rays high power, this effect did not appear for the plasma-exposed sample's crystals.

REFERENCES

1. Montini T, et al. Fundamentals and Catalytic Applications of CeO_2-Based Materials. Chem Rev. 2016;116:5987.
2. Smythe DJ and Brenan JM. Cerium oxidation state in silicate melts: Combined fO_2, temperature and compositional effects. Geochimica et Cosmochimica Acta. 2015;170:173.
3. Graciani J, et al. Highly active copper-ceria and copper-ceria-titania catalysts for methanol synthesis from CO_2. Science. 2014;546:345.
4. Fornasiero P and Dimonte R. Rh-loaded CeO_2-ZrO_2 Solid Solutions as Highly Efficient Oxygen Exchangers: Dependence of the Reduction Behavior and the Oxygen Storage Capacity on the Structural Properties. J Catal. 1995;168:151.
5. Liu Y, et al. Flowerlike CeO_2 microspheres coated with $Sr_2Fe_{1.5}Mo_{0.5}O_x$ nanoparticles for an advanced fuel cell. Sci Rep. 2015;5:11946.
6. Imanaka N, et al. Amorphous Cerium–Titanium Solid Solution Phosphate as a Novel Family of Band Gap Tunable Sunscreen Materials. Chem Mater. 2003;15:2289-2291.
7. Cassee FR, et al. Exposure, Health and Ecological Effects Review of Engineered Nanoscale Cerium and Cerium Oxide Associated with its Use as a Fuel Additive. Cr Rev Toxicol. 2011;213:41.
8. Dai W, Hierarchical CeO_2/Bi_2MoO_6 heterostructured nanocomposites for photoreduction of CO_2 into hydrocarbons under visible light irradiation. Appl Surf Sci. 2018;434:481.
9. Lawrence NJ, et al. Defect Engineering in Cubic Cerium Oxide Nanostructures for Catalytic Oxidation. Nano Lett. 2011;11:2666.
10. Feng XD, et al. Converting ceria polyhedral nanoparticles into single crystal nano spheres. Science. 2006;312:1504.
11. Seo J, et al. Control of adhesion force between ceria particles and polishing pad in shallow trench isolation chemical mechanical planarization. J Nanosci Nanotechno. 2014;14:4351.
12. Campbell CT and Peden CH. Oxygen vacancies and catalysis on ceria surfaces. Science. 2005;309:713.
13. Lykaki M, et al. Ceria nanoparticles shape effects on the structural defects and surface chemistry: Implications in CO oxidation by Cu/CeO_2 catalysts. Applied Catalysis B: Environmental. 2018;18:230.
14. Esch F, et al. Electron localization determines defect formation on ceria substrates. Science. 2005;752:309.
15. Dutta P, et al. Concentration of Ce^{3+} and oxygen vacancies in cerium oxide nanoparticles. Chem Mater. 2006;18:5144.
16. Gupta A, et al. Controlling the surface chemistry of cerium oxide nanoparticles for biological applications. J Mater Chem. 2016;4:3195.

e-ISSN: 2321-6212
p-ISSN: 2347-2278

17. Das S, et al. Seal Cerium oxide nanoparticles: applications and prospects in nanomedicine. Nanomedicine. 2013;8:26.

18. Xu C and Qu X, Cerium oxide nanoparticle: a remarkably versatile rare earth nanomaterial for biological applications. NPG Asia Materials. 2014;6:90.

19. Chen BH and Inbaraj BS, Various physicochemical and surface properties controlling the bioactivity of cerium oxide nanoparticles. Crit Rev Biotechnol. 2018;1.

20. Kim CK, et al. Ceria nanoparticles that can protect against ischemic stroke. Angewandte Chemei International Edition. 2012;51:11039.

21. Gao Y, et al. Cerium oxide nanoparticles in cancer. Onco Targets and therapy. 2014;7:835.

22. Wason MS, et al. Sensitization of pancreatic cancer cells to radiation by cerium oxide nanoparticle-induced ROS production. Nanomedicine. 2013;558:9.

23. O'Donnell RJ, et al. Daugherty in a patent number,US7128804 B2,(2006).

24. Laroussi M, Interaction of Low Temperature Plasma with Prokaryotic and Eukaryotic cells. In Proceedings of the 61st. Gaseous Electronics Conference, Dallas, TX, USA, American Physical Society. 2008;29.

25. Tanaka H, et al. Plasma Medical Science for Cancer Therapy: Toward Cancer Therapy Using Nonthermal Atmospheric Pressure Plasma. IEEE Trans. Plasma Sci. 2014;3760:42.

26. Ehlbeck J, et al. Low temperature atmospheric pressure plasma sources for microbial decontamination. J Phys D Appl Phys. 2011;44:013002.

27. Laroussi M, et al. Perspective: The Physics, Diagnostics, and Applications of Atmospheric Pressure Low Temperature Plasma Sources Used in Plasma Medicine. J Appl Phys. 020901 2017;122.

28. Tanaka H, et al. Interactions between a plasma-activated medium and cancer cells. Plasma Med. 2016;6:101.

29. Levitt SH, et al. Technical Basis of Radiation Therapy: Practical Clinical Applications. Springer. 2012.

30. Klug HP and Alexander LE, X-ray Differaction Procedures for Polycrystalline and Amorphous Materials. John Wiley and Sons Copyright. 1954.

31. Fava RA. Crystal Structure and Morphology. Academic press copyright 1980:133.

32. Renu G, et al. Development of cerium oxide nanoparticles and its cytotoxicity in prostate cancer cells. Adv Sci Lett. 2012:6;17.

33. Preisler EJ, et al. Stability of cerium oxide on silicon studied by x-ray photoelectron spectroscopy. J Vac Sci Technol. 2001;19:1611.

34. Gilmore G. Practical Gamma-ray Spectroscopy. John Wiley & Sons. 2011.